Journal of Colloid and Interface Science 690 (2025) 137304

Contents lists available at ScienceDirect

Journal of Colloid And Interface Science

journal homepage: www.elsevier.com/locate/jcis

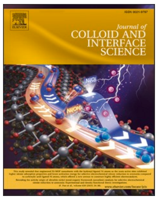

Regular Article

Effect of hydrophilic polymers on the formation of size-controllable aqueous droplets in water-in-oil emulsion and the fabrication of porous micro-silica particles therefrom

Seung-Yeon Kim [a,b], Jin-Woo Jeong [a], A-Jin Kim [a,c], Young-Ran Lee [a], Hye Sun Lee [a], Kangwon Lee [b,*], Seong-Joong Kim [a,*]

[a] *Bio-Convergence R&D Division, Korea Institute of Ceramic Engineering and Technology (KICET), 202 Osongsaengmyeong 1-ro, Osong-eup, Heungdeok-gu, Cheongju-si, Chungcheongbuk-do, Republic of Korea*
[b] *Department of Applied Bioengineering, Seoul National University, 145 Gwanggyo-ro, Yeongtong-gu, Suwon-si, Gyeonggi-do, Republic of Korea*
[c] *Department of Chemical Engineering, Chung Buk National University, Chungdae-ro 1, Seowon-gu, Cheongju, Chungbuk 28644, Republic of Korea*

HIGHLIGHTS

- Porous micro-silica particles were synthesized via emulsion process with hydrophilic polymers.
- The synthesis conditions were varied in terms of type, molecular weight, and concentration of polymers.
- The porous micro-silica particles were controllable in a size range of 1–30 μm.
- The pore size of silica particles could be adjusted from mesopore to macropore.

GRAPHICAL ABSTRACT

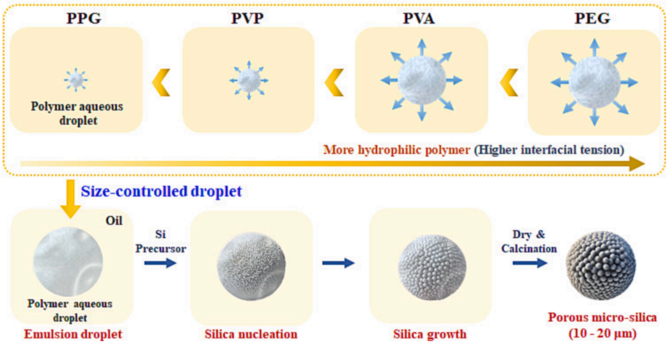

ARTICLE INFO

Keywords:
Water-in-oil (W/O) emulsion
Polymer-water droplet
Hydrophilic polymer
Interfacial tension
Porous microsilica

ABSTRACT

Size-controllable droplets were formed in a water in oil (W/O) emulsion using only hydrophilic polymers without a surfactant to fabricate porous micro-silica particles larger than 20 μm. Droplets of various size ranging from 1 to 30 μm were prepared by emulsifying aqueous solutions containing four types of polymers, namely polyethylene glycol (PEG), polyvinyl alcohol (PVA), polyvinylpyrrolidone (PVP), and polypropylene glycol (PPG), in a pentanol oil phase. Following the addition of tetraethyl orthosilicate (TEOS) as a silica precursor, silica particles were grown via hydrolysis and condensation reactions. The silica particle size depends on the degree of hydrophilicity of the polymers, which determines the interfacial tension between the water droplets and oil. Micro-silica particles >20 μm were obtained from PEG-based emulsion droplets. Notably, the distribution and stability of silica particles can be optimized by controlling the molecular weight and concentration of the hydrophilic polymer. A porous silica structure was successfully obtained by decomposing the residual polymer via an appropriate calcination process. The most uniform and stable porous micro-silica particles with an average size of 20 μm were obtained from an emulsion containing 5 wt% PEG (molecular weight: 4000) after calcination

---

[*] Corresponding authors.
E-mail addresses: kangwonlee@snu.ac.kr (K. Lee), sjkim@kicet.re.kr (S.-J. Kim).

https://doi.org/10.1016/j.jcis.2025.137304
Received 4 November 2024; Received in revised form 8 March 2025; Accepted 10 March 2025

at 500 °C. This novel process enables the eco-friendly synthesis of porous micro-silica particles using only hydrophilic polymer without a surfactant and control of pore size and particle size of >20 μm.

1. Introduction

Silica is widely used as an essential material in numerous applications in a variety of industries. For example, porous silica, which has a high surface area and pore structure, has been employed in a diverse range of fields such as drug delivery systems [1,2], catalysts [3,4], adsorbents [5], and chromatography [6,7]. In the pharmaceutical and catalytic industries, porous silica improves drug delivery, release, and reaction efficiency [8,9]. Environmental engineering plays an important role in the adsorption and removal of pollutants [10,11]. Chromatography allows efficient separation and purification for specific applications, including pharmaceutical production, vaccine development, and biochemical analysis [12–14]. Consequently, the demand for porous silica has continuously increased.

Two features, namely monodispersity and precise control of silica particle size, are particularly important for silica applications [15–17]. Monodispersity means that all particles have a similar size, which helps ensure consistent behavior in biological systems. Monodispersity is particularly important when attempting to achieve predictable drug release and therapeutic effects. Uniformly sized silica particles can be well-distributed in the body, which increases their likelihood of reaching the target area and delivering efficient therapy. The high uniformity of silica particle size not only improves the efficiency of drug delivery, but also enhances reproducibility and reliability [18–21].

The required size of the prepared silica particles varies depending on the application field [22,23]. For example, for therapeutic applications, nanosized particles are desirable for maximizing the effectiveness of a drug because they can easily penetrate the body and selectively target specific tissues [24,25]. In contrast, for chromatography, nanosized particles may lead to a pressure drop, reducing the separation efficiency [26]. Instead, the separation efficiency can be enhanced using a relatively large particle size [13,14,27]. Therefore, for such applications, it is necessary to synthesize large (or at least microscale) silica particles.

Researchers have used various methods to synthesize silica particles, including sol–gel [28–30], seed growth [31–33], emulsion [34,35], and polymer-induced colloid aggregation (PICA) [36,37] methods. Among these, the sol–gel process is the most representative and effective method for synthesizing monodisperse spherical silica particles [38,39]. This synthesis process involves hydrolysis and condensation reactions with a silica precursor under acid or basic conditions, to generate silica particles ranging from 0.05 to 2 μm [40]. Wang et al. investigated the effects of precursors, ammonia, and water on the silica particle size and distribution using the Stöber process and synthesized silica nanoparticles with sizes ranging from 30 to 1000 nm [8]. However, researchers have been unable to synthesize silica particles larger than 1 μm with the Stöber method [41]. To overcome this limitation, the seed growth method, which involves introducing small seed particles into an ammonia solution, followed by a reaction with a silica precursor, has been employed to form larger, uniform particles [31,42]. Giesche et al. successfully synthesized 3.6-μm silica particles via the seed growth process by continuously adding a mixture of alcohol and precursor into the growth solution [32]. In addition, 7 μm silica particles were obtained by adjusting the injection rate of the precursor and adding electrolytes [43].

Another well-known silica particle synthesis method is emulsification. An emulsion is formed in an oil (W/O) or a water (O/W) phase and stabilized with surfactants [44]. An emulsion served as a template for synthesizing silica particles using a silica precursor. The size and morphology of the resulting silica particles can be effectively tailored by adjusting the water droplet size in the emulsion and varying other conditions such as the type of surfactant, reagent concentration, and reaction time [14]. Notably, the inclusion of surfactants or polymers during the synthesis can induce a porous silica particle structure [45]. Monodisperse silica particles can be obtained by emulsification using nonionic surfactants and silica precursors. Compared with other approaches, the emulsion method is a relatively simple process and does not require special equipment; thus, it is an effective way to synthesize silica particles for applications in various industries [44,46].

The emulsion method can also be used to prepare microsized silica particles. Spherical silica particles with an average diameter of 3.6 μm were synthesized in a water-in-oil (W/O) emulsion containing surfactants [47]. The effect of synthesis time on the morphology of the silica particles was further investigated, and micro-sized silica particles in a size range of 5.4–8.2 μm were obtained [48].

However, relatively few studies have been conducted on the synthesis of microsized silica particles using an emulsion process. In addition, research on the preparation of porous silica particles larger than 10 μm are limited. Surfactants are typically employed in emulsion processes to produce monodisperse silica; however, this may lead to experimental complexity and environmental issues during the surfactant removal process [49].

This study proposes a relatively eco-friendly method to synthesize porous silica particles in the size range of 10–20 μm using non-toxic hydrophilic polymers instead of surfactants. Porous silica was synthesized using an in situ emulsion process. In addition, the effects of the type, concentration, and molecular weight of the hydrophilic polymers on the size and distribution of the silica particles were investigated. After removing the polymers by thermal degradation, the pore structures of the resulting porous silica particles were examined.

2. Experimental

2.1. Materials

Tetraethyl orthosilicate (TEOS; 98 %) was used as the silica precursor. 1-Pentanol (99 %) served as the oil phase, and polyethylene glycol (PEG) of various molecular weights (molecular weight: 4000, 10,000, and 20,000) was used as a porogen as well as a stabilizer for the emulsion structure. Polyvinyl alcohol (PVA; molecular weight: 300,000–50,000), polyvinylpyrrolidone (PVP; molecular weight: 40,000), and polypropylene glycol (PPG; molecular weight: 425) were employed as other hydrophilic polymer candidates. These materials were purchased from Sigma-Aldrich. Absolute ethanol (99.9 %, DUKSAN) was used as the solvent, and ammonium hydroxide (25 %, Merck) served as the catalyst. All the chemicals were used without further purification. Deionized water was obtained using a Milli-Q Plus system.

2.2. Preparation of porous micro-silica using an emulsion method

Porous microsilica was prepared by an emulsion method with 1-pentanol, hydrophilic polymers (PEG, PVA, PVP, and PPG), ethanol, ammonium hydroxide, and TEOS. In particular, various molecular weights and concentrations of PEG were used to observe their effects on the properties of the silica particles.

To prepare polymer solutions, a specific concentration of the polymer was dissolved in 10 ml of deionized water, followed by stirring at 400 rpm for 1 h. In the case of the PVA polymer solution, unlike the procedure for the PVP, PPG, and PEG polymers, an additional heating process was carried out at 80 °C for 2 h to completely dissolve the polymer. The polymer solution (1 ml) was then added to 7 ml of 1-pentanol. The mixture was manually shaken vigorously for 20 s to obtain a homogeneous emulsion. Ethanol, ammonium hydroxide, and TEOS (0.5

ml each) were sequentially added to the emulsion (Fig. S1), followed by thorough shaking by hand for 20 s at each stage (Fig. S2). The mixture was left to stand for 12 h to allow the growth of silica particles from the droplets formed in the emulsion via hydrolysis and condensation reactions (Fig. S3). Following the reaction, the mixture was poured onto a ceramic plate and dried in an oven at 70 ℃ for 3 h. The dried powder was calcinated at temperatures of 400–600 ℃ for 2 h at a ramping rate of 1 ℃/min to remove the residual polymer. Detailed synthesis conditions are listed in Table 1.

2.3. Characterization

The morphologies of the porous microsilica particles were examined using scanning electron microscopy (SEM; COXEM-EM30N) at an accelerating voltage of 20 kV. An optical microscope (Primovert, ZEISS) was used to observe the size and shape of the droplets formed in the emulsion.

A thermogravimetric analysis (TGA; SDT Q600) and a differential thermal analysis (TGA/DTA, NETZSCH STA 409 PC/PG) were conducted to examine the thermal properties of the silica particles. First, a platinum crucible containing 10 mg of the sample was subjected to increasing temperature at a rate of 10 ℃/min, reaching a maximum of 800 ℃ under a flow of air.

Brunauer–Emmett–Teller (BET) specific surface areas and pore volumes were measured via N_2 adsorption (Micromeritics ASAP 2460). The pore size distribution was calculated using the Barrett–Joyner–Halenda (BJH) and nonlocal density functional theory (NLDFT; equilibrium model N_2 @ 77 K on silica (cylindrical pores)) methods. Prior to the analyses, the samples were degassed at 200 ℃ for 10 h.

Fourier transform infrared (FT-IR) spectroscopy (SP8000, PerkinElmer) was used to analyze the chemical structure of the samples over a spectral range of 4000–600 cm^{-1}. The dried samples (2 mg) were finely powdered and mixed with KBr (230 mg). The silica-KBr mixture was compressed at a pressure of 9–10 bar to produce transparent pellets. The obtained spectra were evaluated to determine the functional groups and chemical bonding properties.

X-ray diffraction (XRD) analyses were performed to investigate the silica structure after being calcined at different temperatures (400, 500, and 600 ℃). XRD was used to analyze the crystalline structure, phase composition, and potential changes in the crystallinity of silica as a function of the calcination temperature. XRD patterns of the silica powder were recorded using a Rigaku D/Max-2200 V diffractometer equipped with a Cu tube and graphite monochromator at 40 kV.

Table 1
Various conditions employed for silica synthesis via emulsion method.

Sample	Polymer[wt.%]				Molecular Weight (Da)	Calcination Temperature (℃)
	PPG	PVP	PVA	PEG		
1 (Fig. 3 (a))	5				425	500
2 (Fig. 3 (b))		5			40,000	500
3 (Fig. 3 (c))			5		30,000–50,000	500
4 (Fig. 3 (d))				5	4000	500
5 (Fig. 5 (c))				5	10,000	500
6 (Fig. 5 (d))				5	20,000	500
7 (Fig. 7 (a))				3	4000	500
8 (Fig. 7 (c))				7	4000	500
9 (Fig. 8 (c))				5	4000	400
10 (Fig. 8 (c))				5	4000	600

* Other additives: EtOH (0.5 ml), ammonium hydroxide (0.5 ml), and 0.5 ml TEOS.

Viscosity was measured at 25 ℃ using a viscometer (LVDV2 + Pro, Brookfield) equipped with an SCP-18 spindle. The interfacial tension between the polymer aqueous solution and oil phase was measured using a contact angle measuring system (KRUSS, DSA 100). The microsilica particle size was analyzed using a particle size analyzer (PSA; LA-960, Horiba). Transmission electron microscopy (TEM) images of the microsilica particles were obtained using a Jeol JEM-2100Plus transmission electron microscope operating at 200 kV.

3. Results and discussion

3.1. Morphology of the emulsion droplets derived from hydrophilic polymers with different molecular weights and concentrations

Fig. 1(a) shows the optical microscopy images of the emulsions formed by dispersing an aqueous polymer solution in an oil (pentanol) phase using different polymers (PPG, PVP, PVA, and PEG). The formation mechanism of the porous microsilica particles via the emulsion method is shown in Fig. S4. The polymer concentrations of all the samples were maintained at 5 wt%. The largest droplet size was observed in the emulsion dispersed in the PEG aqueous solution, whereas PPG and PVP formed relatively smaller droplets. This is attributed to the different hydrophilic properties of the polymers, which affect the droplet size in the emulsion by altering the interfacial energy between the water and oil phases (Table S1) [50,51].

The interfacial tensions of the polymer aqueous solutions in oil were as follows: PEG (35.8 mN/m) > PVA (25.1 mN/m) > PVP (8.63 mN/m) > PPG (7.57 mN/m). The hydrophilicities of PPG and PVP were lower than those of PEG and PVA; this affected the amphiphilic characteristics of the water and oil phases, leading to smaller droplet sizes by substantially reducing the interfacial tension (Fig. 2) [52–54].

In particular, the smallest droplet size was observed in the emulsion dispersed in the PPG aqueous solution, which had the lowest hydrophilicity among the four polymers and interacted the most with pentanol. In contrast, PEG and PVA, which had better hydrophilic properties, produced larger droplets by maintaining or slightly lowering the interfacial energy without coalescence or flocculation.

Droplets prepared without a hydrophilic polymer tended to easily combine with each other (coalescence) owing to high interfacial tension, forming irregular and excessively large droplets (Fig. S5) [55–57]. Consequently, the relatively amphiphilic PPG and PVP were critical for the formation of smaller droplets in the emulsion, whereas the highly hydrophilic PEG and PVA contributed to the development of larger droplets. Varying the hydrophilicity of the polymer enabled control of the droplet size in the emulsion from sub-micrometers to tens of micrometers.

It was also confirmed that employing a hydrophilic polymer resulted in a stable emulsion that was effective in forming and stabilizing emulsion droplets.

Fig. 1(b) shows the optical microscopy images of droplets of an aqueous solution dispersed in an oil phase according to the molecular weight of PEG. For PEG 200, the droplet size was very small at about 2 µm, and it had a non-uniform size distribution with a range of 1–5 µm. In contrast, droplets of 20–30 µm were observed in the emulsions derived from PEG 4000, 10,000, and 20,000. This can be attributed to the differences in the viscosities of the polymers according to their molecular weights (Table S1). The viscosity of the aqueous solution increased as the molecular weight of PEG increased (Fig. 3(a)).

High-viscosity polymer aqueous solutions appeared to suppress the formation of small droplets and stabilize large droplets within the emulsion. The long chains of high-molecular-weight polymers cause entanglements between chains, which become more severe with higher molecular weights, lowering the fluidity of the solution and increasing

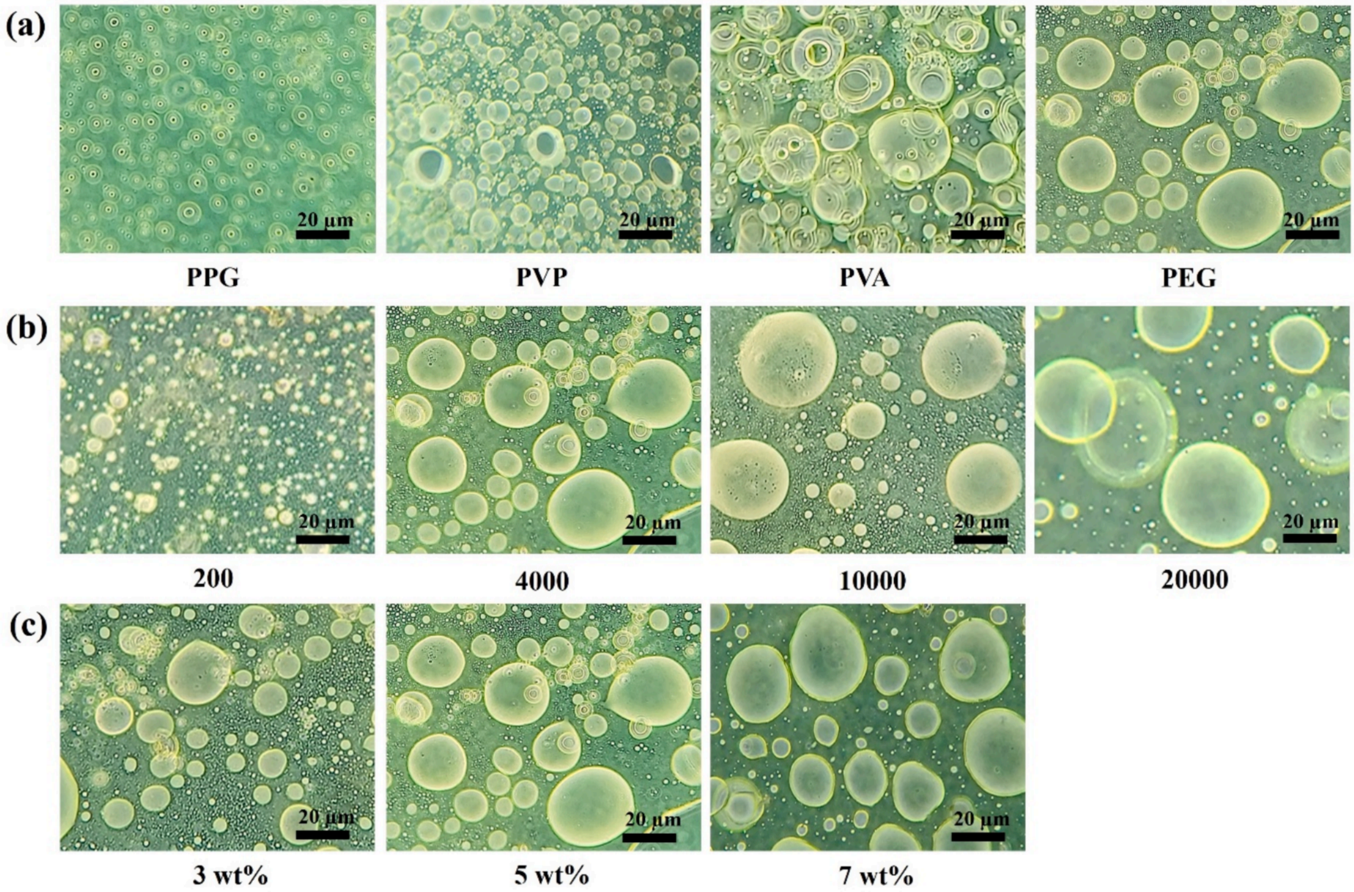

Fig. 1. Optical microscope images of emulsion droplets prepared with (a) different polymers (PPG, PVP, PVA, and PEG (5 wt% PEG 4000)), (b) different molecular weight of PEG (200, 4000, 10,000, and 20,000 (Conc.: 5 wt%)), and (c) different PEG concentration (3, 5, and 7 wt% (molecular weight: 4000)).

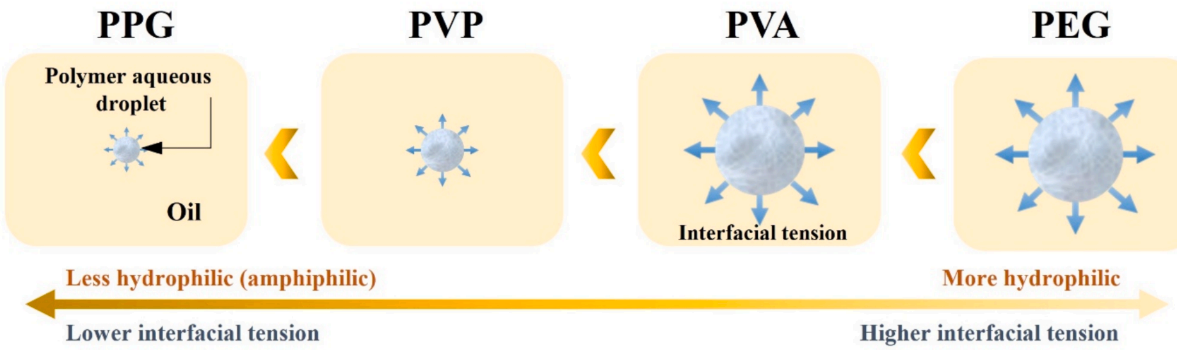

Fig. 2. Schematic illustration of droplet formation in emulsion with various hydrophilic polymers.

viscosity. This interaction lowers the activity of droplets in the emulsion, thereby limiting the formation of small droplets.

In contrast, a low-viscosity aqueous solution allows the formation of small droplets. Therefore, the emulsion derived from PEG 200 formed small droplets owing to the low viscosity of the aqueous solution, whereas the high-viscosity emulsions of PEG 4000, 10,000, and 20,000 formed large droplets.

However, polymers with low interfacial tension, such as PPG and PVP, did not form large droplets, despite increased viscosity (Table S1 and Fig. S6). Therefore, both the interfacial tension and viscosity of the solution simultaneously control the size of the droplets in emulsions based on hydrophilic polymer aqueous solutions.

Fig. 1(c) shows the optical microscope images of the droplets in the emulsion according to the PEG concentration. The emulsion droplets prepared with an aqueous solution containing 3 wt% PEG resulted in a relatively small average droplet size of 10 μm. For the emulsion formed with 5 wt% PEG, the droplet size tended to increase to about 15–20 μm, while, the droplet size achieved with 7 wt% PEG exceeded 20 μm.

Generally, the addition of a polymer to an emulsion affects the interfacial energy of the resulting polymer aqueous solution. Even when the polymer is highly hydrophilic, the polymer chains can interfere with hydrogen bonding between the water molecules in the droplets, which decreases the water–oil interfacial tension [58]. This decrease in the interfacial tension eventually reduces the emulsion droplet size.

However, in this study, the droplet size increased despite an increase in polymer concentration. This can be attributed to the increase in the

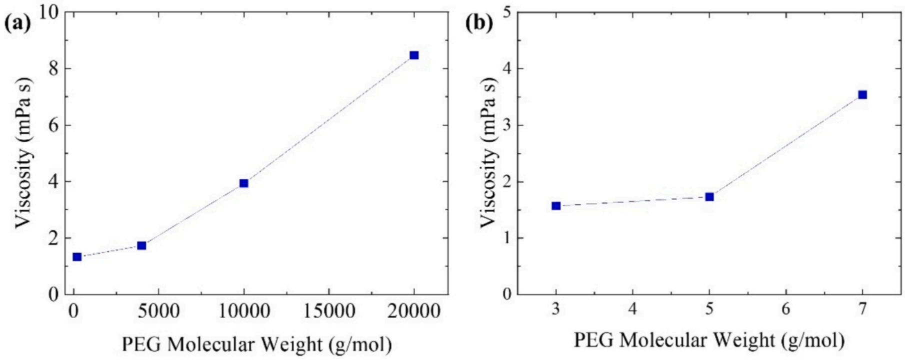

Fig. 3. Viscosity of PEG aqueous solutions prepared with different (a) polymer molecular weights and (b) concentrations (viscosity of water: 0.87 at 25 ℃; the number of repetitions of the experiments: 3, and error estimates: 4.2 %).

viscosity of the aqueous solution with increasing PEG concentration (Fig. 3(b)), which is similar to the trend observed with increasing polymer molecular weight (Fig. 1(b)). A higher PEG concentration causes the polymer chains to become more entangled in the solution. Furthermore, the polymer occupies more space in the solution, which hinders the flow of the solution and increases its viscosity.

In particular, the viscosity of the aqueous solution with 7 wt% PEG increased rapidly, resulting in large droplets with size exceeding 20 μm.

3.2. *Morphology of porous micro-silica particles derived from hydrophilic polymers with different molecular weights and concentrations*

Fig. 4(a) presents SEM images of the micro-silica particles derived from emulsions based on the four polymers. The micro-silica particles were observed after calcination at 500 ℃, and all the samples showed significantly different particle sizes (Fig. 5(a)). In this study, particle size indicates the diameter of spherical silica. The silica particles derived from PPG had a relatively small size in the range of 1–8 μm, with an irregular morphology. The silica particles derived from PVP showed a slightly more uniform structure than that of PPG but still exhibited a broad size distribution and particle size as small as 7 μm. In contrast, the PVA and PEG-based silica particles were relatively uniform and spherical with average sizes of approximately 15 and 20 μm, respectively. A slightly larger particle size was observed for the PEG-based silica.

These trends were consistent with the droplet size results shown in Fig. 1(a). The initial droplet size played a critical role in determining the final size of the silica particles. The hydrolysis and condensation reactions were initiated as soon as the silica precursor penetrated the

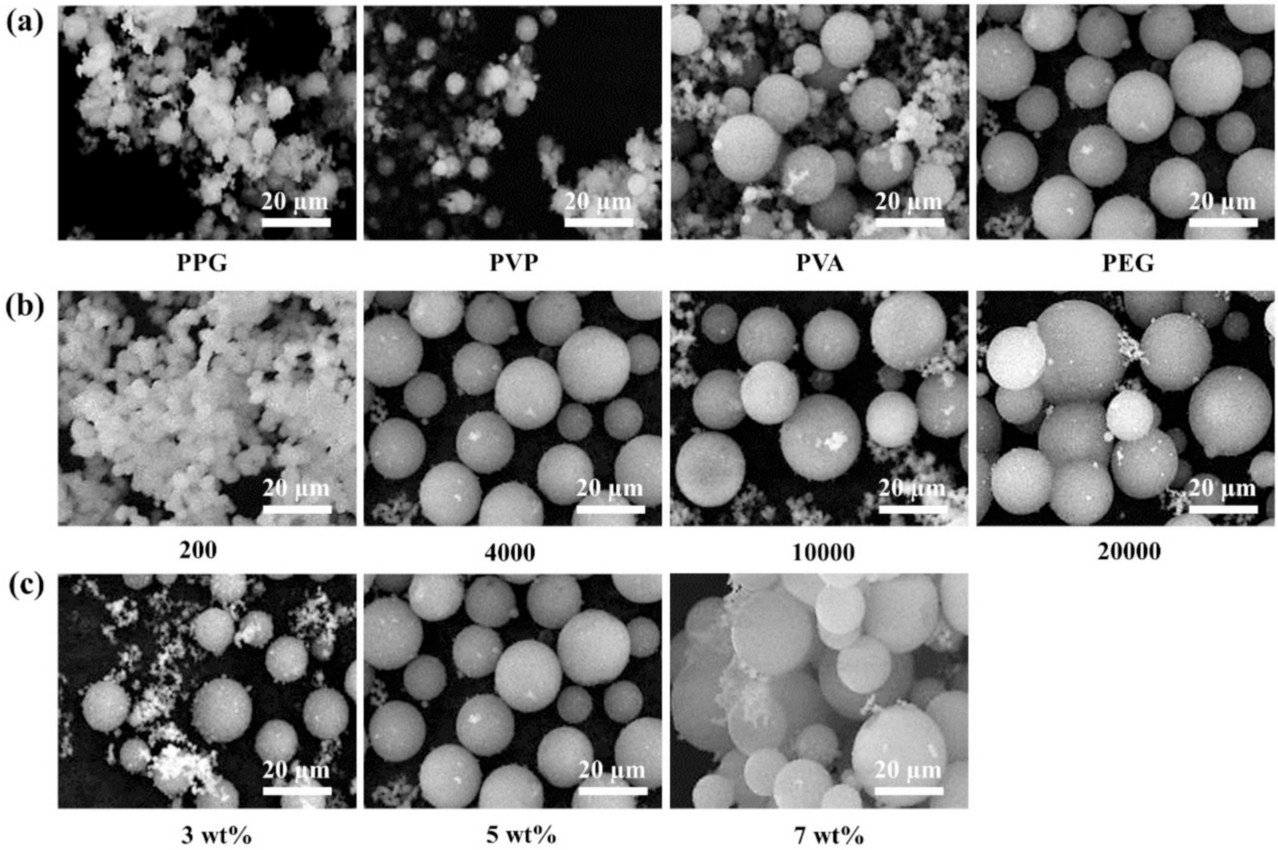

Fig. 4. SEM images of silica synthesized with different (a) polymers (PPG, PVP, PVA, and PEG (W. 4000; Cal. Temp. 500 ℃)), (b) PEG molecular weights (200, 4000, 10,000, and 20,000 (Conc. 5 wt%; Cal. Temp. 500 ℃)), and (c) PEG concentration (3 wt%, 5 wt%, and 7 wt% ((M.W. 4000; Cal. Temp. 500 ℃)).

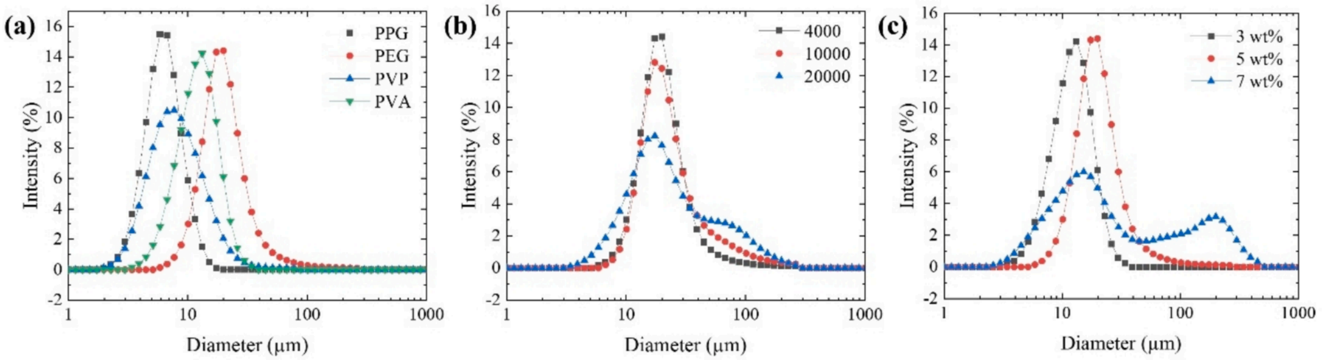

Fig. 5. Particle size distribution of the silica synthesized with different (a) polymers (PPG, PVP, PVA, and PEG (molecular weight: 4000; Cal. Temp.: 500 ℃)), (b) PEG molecular weights (200, 4000, 10,000, and 20,000 (Conc.: 5 wt%; Cal. Temp.: 500 ℃)), and (c) PEG concentration (3, 5, and 7 wt% ((molecular weights: 4000; Cal. Temp.: 500 ℃)).

emulsion droplets. Subsequently, silica particles formed by the consumption of water in the droplets [44]. Consequently, the nucleation and growth of silica proceeds only in the droplets, and the final size of the silica particles is determined by the droplet size.

However, after synthesis, the microsilica particles were slightly smaller than the emulsion droplets. This is thought to occur because the silica density (general amorphous silica density is 2.2 g/cm^3) is higher than that of the TEOS (0.9 g/cm^3), resulting in particle shrinkage. Therefore, to obtain silica particles with sizes in the order of tens of micrometers, it is critical to initially form a large droplet. Among the four hydrophilic polymers, PEG was the most appropriate for producing large and uniform microsilica particles. Further experiments were performed using PEG as the hydrophilic polymer additive for the aqueous solution in the emulsion.

Fig. 4(b) presents SEM images of the silica particles synthesized with different molecular weights of PEG (200, 4000, 10,000, and 20,000). A distinct difference in the microsilica particle size according to the molecular weight was observed (Fig. 5(b)). The size of the silica particles prepared with PEG200 was approximately 2 μm. This can be attributed to the small size of the emulsion droplets formed from the low-viscosity aqueous solution, as shown in Fig. 1(b). The small droplets in the emulsion prepared with the low-molecular-weight polymer formed small particles, similar to the results with different types of polymers, as indicated in Fig. 4(a).

Conversely, the sizes of the silica particles synthesized from PEG 4000, 10,000, and 20,000 were significantly larger, resulting in spherical porous silica particles larger than 10 μm. Uniform and relatively large droplets formed in the emulsion upon increasing the viscosity of the aqueous solution using high-molecular-weight PEG (Fig. 1(b)), which enabled the silica particles to effectively grow into large particles.

Nevertheless, the particle size distributions of the silica particles prepared with PEG 10,000 and 20,000 tended to be somewhat broad, even though the increase in the molecular weight was advantageous for the formation of large silica particles. Excessively high aqueous solution viscosity appeared to hinder the formation of uniform droplets. Furthermore, the viscosity rapidly increased with PEG molecular weights of 10,000 or more (Fig. 3(a)). Therefore, PEG 4000 was determined to be the optimal molecular weight for obtaining microsilica particles with the most uniform and desirable size.

Fig. 4(c) presents SEM images of silica synthesized with PEG concentrations of 3, 5, and 7 wt%. As the PEG concentration increased, the number of small silica particles (1–2 μm) decreased noticeably, and the overall particle size increased. This can be attributed to the increased viscosity of the aqueous solution at higher PEG concentrations, as shown in Fig. 1(c). The smallest silica particles were formed with 3 wt% PEG, which had the lowest viscosity, and a non-uniform particle distribution was observed. In contrast, for 5 wt% PEG, uniform silica particles of 20 μm in size (Fig. 5(c)) were realized owing to an appropriate balance between the increase in viscosity and decrease in interfacial tension.

Even though the silica particle size increased remarkably at 7 wt% PEG (exceeding 25 μm), the particle size distribution was broad. The addition of too much polymer can hinder the formation of a uniform and stable emulsion owing to an excessive reduction in interfacial tension (water–oil phase) and an increase in viscosity (aqueous solution). In addition, some aggregation of the microsilica particles was observed at 7 wt% PEG, as shown in the SEM images in Fig. 4(c). This led to a bimodal particle-size distribution of the silica particles, as shown in Fig. 5(c). Adding excessive amounts of PEG allows more PEG molecules to be present on the droplet surface, facilitating interactions such as hydrogen bonding between the PEG molecules during the silica growth process. Accordingly, a PEG concentration of 5 wt% was determined to be optimal for the formation of uniform and large microsized silica particles.

Consequently, several factors are critical during silica synthesis via the emulsion method, such as adjusting the polymer concentration, molecular weight, and type of polymer added to the emulsion. These variables should be carefully considered to achieve the desired microsilica particle size and distribution. Furthermore, the narrowest particle size distribution was obtained for sample 4 (5 wt% PEG 4000), whose d90/d10 value was 2.5. Although this was not a monodisperse size distribution, the new synthesis method in this study seems to be a good process to prepare silica particles larger than 10 μm with a d90/d10 value of 2.5.

3.3. *Effect of calcination temperature on porous micro-silica particle properties*

The thermal properties of the micro-silica particles prepared with 5 wt% of PEG 4000 were observed up to 800 ℃ via TGA, as shown in Fig. 6(a). The decomposition temperature and weight ratio of the organic substances in the microsilica particles were investigated in air. The initial weight loss at 100 ℃ was assigned to the evaporation of water. Thereafter, lasting weight loss was observed between 150 and 500 ℃. The decomposition of the PEG polymer began at 150 ℃ and rapidly decreased up to 200 ℃. The remaining PEG gradually decomposed above 200 ℃, and it was completely decomposed at 500 ℃. This indicates that the polymer can be completely removed at a calcination temperature of at least 500 ℃. The total weight loss at 600 ℃ was approximately 25 %, indicating the porous structure of the micro-silica particles. More detailed thermal properties of the microsilica particles are shown in Fig. S7.

The functional groups of the synthesized silica were investigated according to the calcination temperature via an FT-IR analysis (Fig. 6(b)). Silica particles synthesized with 5 wt% PEG 4000 were prepared at

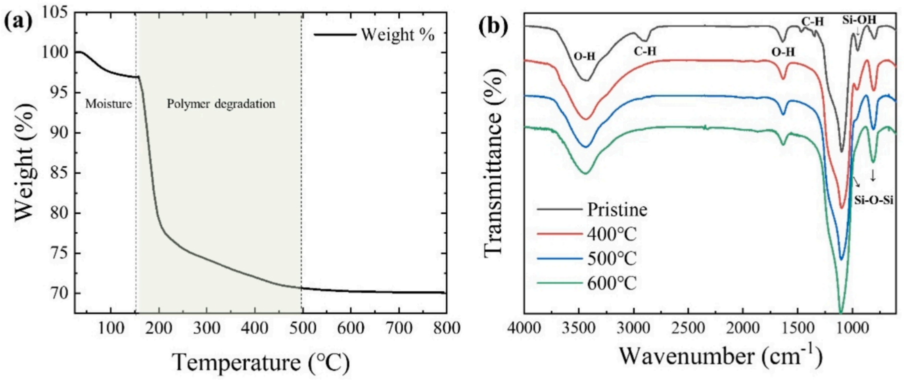

Fig. 6. (a) TGA curve of the synthesized micro-silica particles prior to calcination and (b) FT-IR spectra of silica before and after calcination.

a sintering temperature of 400–600 ℃. The peaks assigned to 764 and 1052 cm^{-1} indicate the Si—O—Si symmetric and asymmetric stretching vibrations, respectively. Si—OH and OH groups appeared at 966 and 3300 cm^{-1}, respectively. The C—H group of PEG was observed at 1341, 1460, and 2890 cm^{-1}. The Si—OH and Si—O—Si groups appeared simultaneously in the synthesized silica particles owing to the hydrolysis and condensation reactions prior to calcination. The Si—OH peak gradually decreased with increasing calcination temperature, whereas the Si—O—Si peak became stronger. This indicates that most of the Si—OH groups obtained by hydrolysis were converted to Si—O—Si groups during calcination. In addition, the C—H group of PEG was not observed in the calcined silica, indicating that PEG was removed during the calcination process. Furthermore, the number of OH groups continuously decreased with increasing calcination temperature. This can be attributed to the conversion of Si—OH to Si—O—Si, as well as the decomposition of PEG-containing OH groups. Nevertheless, strong O—H peaks were also observed in all samples owing to the presence of water in KBr and silica.

The SEM images of the microsilica particles calcined at different temperatures are presented in Fig. S8.

3.4. *Pore size properties of porous micro-silica particles*

Fig. 7 shows the pore distributions of the porous microsilica particles synthesized in this study. Interestingly, a bimodal mesopore distribution was observed in the 2–10 and 10–200 nm regions. During silica synthesis, numerous silica nuclei were simultaneously formed and grown within the droplet, leading to a mesoporous structure. A more detailed pore size distribution in the small-sized region (2–10 nm), obtained using the NLDFT model, is presented in Fig. S9. As shown in Figs. 8 and S10, porous microsilica particles were formed by the aggregation of numerous silica nanoparticles with sizes ranging from 10 to 100 nm into a spherical shape. Consequently, the pores in the range of 2–200 nm were determined by analyzing the spacing between the silica nanoparticles. A detailed schematic illustration of the pore formation mechanism in porous microsilica is shown in Fig. 9.

The distribution of the pore sizes in the prepared microsilica particles according to the PEG molecular weight is shown in Fig. 7 (a). With an increase in the molecular weight, the pore volume in the small pore region (2–10 nm) decreased slightly, while that in the large pore region (10–200 nm) increased. In particular, the pore size increased noticeably in the 10–200-nm region. A higher molecular weight increases the resistance to fluidity because of greater entanglement between the polymer molecules or chains, leading to an increase in droplet viscosity (Fig. 3(a)). This can interfere with the uniform and fine dispersion of the polymer between the silica nanoparticles formed in the droplets, resulting in the formation of nonuniform and somewhat large pores.

No remarkable change in the pore size was observed in the small region. The specific surface areas and pore volumes of the porous microsilica particles are listed in Table 2. Both were reduced by increasing the molecular weight, owing to the increase in pore size and reduction in mesopores. In particular, the pore volume decreased owing to the stronger interactions between the polymer chains with higher molecular weights. The BET adsorption–desorption curves are shown in Fig. S12.

Fig. 7(b) shows the pore size distributions of the microsilica particles synthesized with different PEG concentrations. As the PEG concentration increased, a change in pore volume was observed in the small pore size region (2–10 nm), whereas the pore size in the large pore region (10–200 nm) increased. As mentioned above, the PEG polymer remained between the small silica nanoparticles in the droplets during the growth process, and the pore size was determined after calcination. Therefore, a higher polymer concentration can result in the formation of a larger pore structure, because more polymer is contained between the

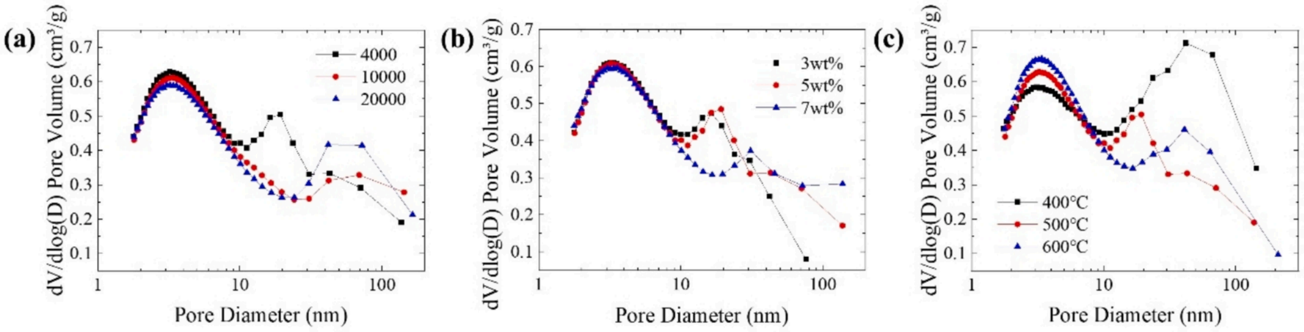

Fig. 7. Pore size distribution of synthesized porous micro-silica particles with different (a) PEG molecular weight (Conc.: 5 wt%; Cal. Temp.: 500 ℃), (b) PEG concentration (molecular weight: 4000; Cal. Temp. 500 ℃), and (c) calcination temperature (Conc. 5 wt%; molecular weight: 4000).

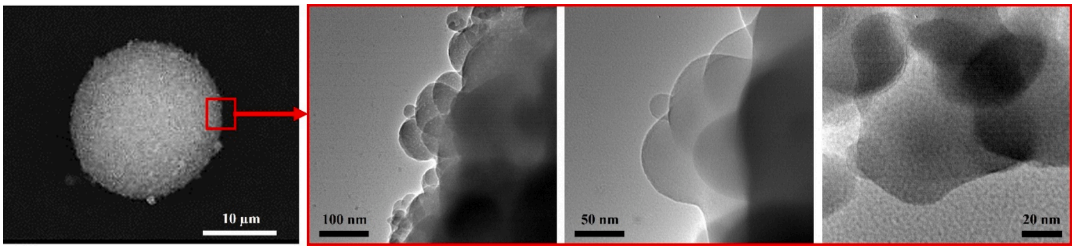

Fig. 8. SEM and TEM images of a porous micro-silica particle synthesized by the emulsion process with hydrophilic polymer (Poly. PEG; Conc. 5 wt%; molecular weight: 4000; Cal. Temp. 500 °C).

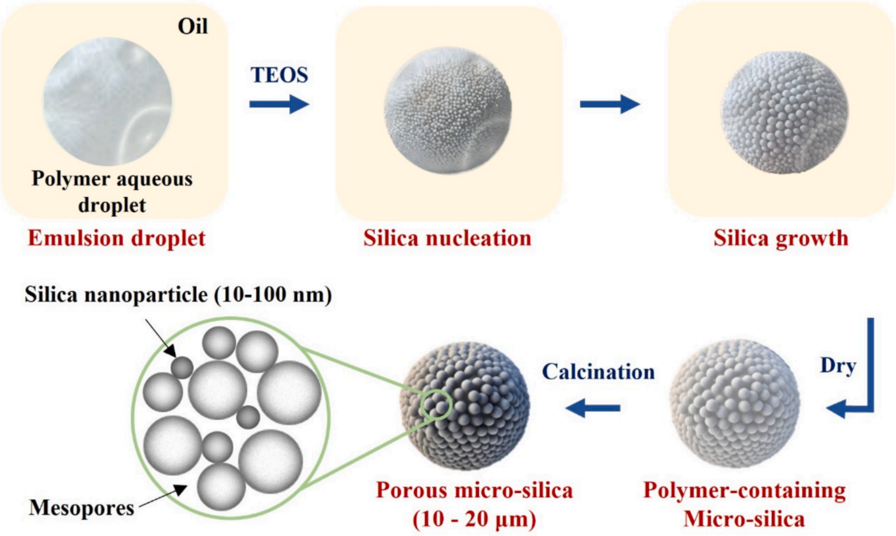

Fig. 9. Schematic illustration of the specific pore formation mechanism in porous micro-silica according to the nucleation and growth of silica nanoparticles in an emulsion droplet.

Table 2
Specific surface area and pore volume of porous micro-silica particles measured by a N_2 adsorption analysis.

Sample		Specific surface area (m^2/g)	Pore volume (cm^3/g)
PEG molecular weight (Da) (Conc. 5: wt%; Cal. Temp.: 500 °C)	4000	542	0.84
	10,000	506	0.71
	20,000	470	0.71
PEG concentration (wt%) (Molecular weight: 4000; Cal. Temp.: 500 °C)	3	540	0.73
	5	542	0.84
	7	465	0.64
Calcination temperature (°C) (Conc.: 5 wt%; Molecular weight: 4000)	400	334	0.74
	500	542	0.84
	600	606	1.04

silica nanoparticles in the droplets. Furthermore, macropores larger than 100 nm were formed, as shown in Fig. 7(b), but their dimensions could not be determined using the BJH method.

Conversely, the specific surface area decreased at higher PEG concentrations owing to the formation of a larger pore structure, whereas the pore volume increased because it contained a larger number of polymers (Table 2). Nevertheless, the microsilica particles prepared with 7 wt% PEG showed a reduced pore volume. This was ascribed to the increase in macropores, which was not reflected in the pore volume results obtained by the BJH analysis.

Fig. 7(c) shows the pore size distribution of the synthesized microsilica particles according to the calcination temperature. The micro-silica particles calcinated at 400 °C had a lower pore volume in the small pore region because the polymer was not completely decomposed, as shown in Figs. 6 (a) and S7. Moreover, the pores did not shrink sufficiently after the decomposition of the polymer because the temperature was low; thus, a relatively large pore structure was observed. As the calcination temperature was raised to 500 °C, the polymer in the micro-silica particles completely decomposed, and the pore volume in the small pore region rapidly increased. In addition, the pore size in the large-pore region decreased owing to shrinkage between the silica nanoparticles. Nevertheless, an enlargement in pore size in the large pore region was observed when silica was calcinated at 600 °C. The silica nanoparticles connected with each other during the calcination process and grew into larger grains, which resulted in larger pores [59]. Simultaneously, the specific surface area and pore volume increased with the calcination temperature (Table 2). This may be due to the significant increase in pore volume in the small-pore region.

These results confirm that controlling various conditions, such as molecular weight, concentration, and calcination temperature, is highly useful for tailoring the pore properties of porous micro-silica.

This study investigated a novel porous microsilica synthesis process in a W/O emulsion in which only a hydrophilic polymer was added without a surfactant. The sizes of the resulting porous microsilica particles were successfully controlled using hydrophilic polymers in a W/O emulsion. Unlike the conventional method, the new silica synthesis method is capable of controlling the particle size in a simple and eco-friendly manner without surfactants. The type, molecular weight, and concentration of the hydrophilic polymers significantly affected the size of the emulsion droplets and resulting silica particles. When four different polymers (PVP, PPG, PVA, and PEG) were used to create the emulsion, they each affected the droplet size differently owing to their different hydrophilic properties, which subsequently changed the interfacial energy between the water and oil phases.

In particular, the silica fabricated with PEG, which is highly hydrophilic, had a relatively large particle size (>20 μm) because it induced the highest interfacial tension. The trend in the initial droplet size was similar to that of the final microsilica particle size. Higher molecular weight polymers resulted in the formation of both larger droplets and micro-silica particles owing to the increased viscosity of the polymer aqueous solutions. In addition, a higher polymer concentration increased the microsilica particle size owing to the increased viscosity, despite a reduction in interfacial tension caused by impeded hydrogen bonding between water molecules. The results show that a proper balance between the viscosity and interfacial tension is critical.

The resulting porous microsilica particles possessed a bimodal pore structure in the range of 2–100 nm or more. The synthesis process proposed in this study enables the pore size of micro-silica particles to be tailored from mesopores to macropores with a high specific surface area of 542 m^2/g.

Porous microsilica has been synthesized using surfactants. Moreover, the synthesis of silica particles larger than 20 μm has seldom been reported. In this study, an emulsion process with hydrophilic polymers enabled the eco-friendly synthesis of porous micro-silica particles without a surfactant. Furthermore, the new controllable silica synthesis process was able to achieve particle sizes exceeding 20 μm. The porous microsilica fabricated in this study can be utilized for separation and purification using column chromatography because the large particles minimize the pressure drop. In future, further studies will be conducted to synthesize porous microsilica particles with better monodisperse size distributions and precise pore size control.

CRediT authorship contribution statement

Seung-Yeon Kim: Writing – review & editing, Writing – original draft, Methodology, Investigation, Conceptualization. **Jin-Woo Jeong:** Validation, Investigation, Formal analysis. **A-Jin Kim:** Investigation, Formal analysis. **Young-Ran Lee:** Project administration, Funding acquisition. **Hye Sun Lee:** Formal analysis. **Kangwon Lee:** Writing – review & editing, Investigation, Conceptualization. **Seong-Joong Kim:** Writing – review & editing, Writing – original draft, Supervision, Project administration, Methodology, Investigation, Funding acquisition, Conceptualization.

Declaration of competing interest

The authors declare that they have no known competing financial interests or personal relationships that could have appeared to influence the work reported in this paper.

Acknowledgments

This research was supported by a grant of the project for The Government-wide R&D to Advance Infectious Disease Prevention and Control, Republic of Korea (grant number: RS-KH140358), the Korea Institute of Ceramic Engineering and Technology (KICET, 2410002182), and the National Research Council of Science & Technology (NST) grant by the Korea government (MSIP) (No. CRC22043-300).

Appendix A. Supplementary data

Supplementary data to this article can be found online at https://doi.org/10.1016/j.jcis.2025.137304.

Data availability

Data will be made available on request.

References

[1] Q. Lei, J. Guo, A. Noureddine, A. Wang, S. Wuttke, C.J. Brinker, W. Zhu, Sol–gel-based advanced porous silica materials for biomedical applications, Adv. Funct. Mater. 30 (41) (2020).

[2] Z. Li, J.C. Barnes, A. Bosoy, J.F. Stoddart, J.I. Zink, Mesoporous silica nanoparticles in biomedical applications, Chem. Soc. Rev. 41 (7) (2012) 2590–2605.

[3] T. da Cunha, A. Maulu, J. Guillot, Y. Fleming, B. Duez, D. Lenoble, D. Arl, Design of silica nanoparticles-supported metal catalyst by wet impregnation with catalytic performance for tuning carbon nanotubes growth, Catalysts 11 (8) (2021).

[4] J.L. Gole, C. Burda, Z.L. Wang, M. White, Unusual properties and reactivity at the nanoscale, J. Phys. Chem. Solid 66 (2–4) (2005) 546–550.

[5] G. Neri, G. Rizzo, C. Crisafulli, L. De Luca, A. Donato, M.G. Musolino, R. Pietropaolo, Isomerization of α-pinene oxide to campholenic aldehyde over Lewis acids supported on silica and titania nanoparticles, Appl. Catal. A 295 (2) (2005) 116–125.

[6] H.T. Khoo, C.H. Leow, Advancements in the preparation and application of monolithic silica columns for efficient separation in liquid chromatography, Talanta 224 (2021).

[7] K. Unger, D. Kumar, M. Grün, G. Büchel, S. Lüdtke, T. Adam, K. Schumacher, S. Renker, Synthesis of spherical porous silicas in the micron and submicron size range: challenges and opportunities for miniaturized high-resolution chromatographic and electrokinetic separations, J. Chromatogr. A 892 (1–2) (2000) 47–55.

[8] Q. He, J. Shi, Mesoporous silica nanoparticle based nano drug delivery systems: synthesis, controlled drug release and delivery, pharmacokinetics and biocompatibility, J. Mater. Chem. 21 (16) (2011).

[9] M. Karimi, H. Mirshekari, M. Aliakbari, P. Sahandi-Zangabad, M.R. Hamblin, Smart mesoporous silica nanoparticles for controlled-release drug delivery, Nanotechnol. Rev. 5 (2) (2016).

[10] M.E. Peralta, D.O. Mártire, M.S. Moreno, M.E. Parolo, L. Carlos, Versatile nanoadsorbents based on magnetic mesostructured silica nanoparticles with tailored surface properties for organic pollutants removal, J. Environ. Chem. Eng. 9 (1) (2021).

[11] S. Zeb, N. Ali, Z. Ali, M. Bilal, B. Adalat, S. Hussain, S. Gul, F. Ali, R. Ahmad, S. Khan, H.M.N. Iqbal, Silica-based nanomaterials as designer adsorbents to mitigate emerging organic contaminants from water matrices, J. Water Process Eng. 38 (2020) 101675, https://doi.org/10.1016/j.jwpe.2020.101675.

[12] Q. Qu, Y. Si, H. Xuan, K. Zhang, X. Chen, Y. Ding, S. Feng, H.Q. Yu, M.A. Abdullah, K.A. Alamry, Dendritic core-shell silica spheres with large pore size for separation of biomolecules, J. Chromatogr. A 1540 (2018) 31–37.

[13] H. Xia, G. Wan, J. Zhao, J. Liu, Q. Bai, Preparation and characterization of monodisperse large-porous silica microspheres as the matrix for protein separation, J. Chromatogr. A 1471 (2016) 138–144.

[14] F. Akhter, A.A. Rao, M.N. Abbasi, S.A. Wahocho, M.A. Mallah, H. Anees-ur-Rehman, Z.A. Chandio, A comprehensive review of synthesis, applications and future prospects for Silica Nanoparticles (SNPs), Silicon 14 (14) (2022) 8295–8310.

[15] L.P. Singh, S.K. Bhattacharyya, G. Mishra, S. Ahalawat, Functional role of cationic surfactant to control the nano size of silica powder, Appl. Nanosci. 1 (3) (2011) 117–122.

[16] W. Liu, W. Wu, C. Selomulya, X.D. Chen, A single step assembly of uniform microparticles for controlled release applications, Soft Matter 7 (7) (2011).

[17] K.-S. Chou, C.-C. Chen, The critical conditions for secondary nucleation of silica colloids in a batch Stöber growth process, Ceram. Int. 34 (7) (2008) 1623–1627.

[18] M.K. Kim, D.H. Ki, Y.G. Na, H.S. Lee, J.S. Baek, J.Y. Lee, H.K. Lee, C.W. Cho, Optimization of mesoporous silica nanoparticles through statistical design of experiment and the application for the anticancer drug, Pharmaceutics 13 (2) (2021).

[19] M. Vallet-Regí, M. Colilla, I. Izquierdo-Barba, M. Manzano, Mesoporous silica nanoparticles for drug delivery: current insights, Molecules 23 (1) (2017) 47.

[20] B. Ma, L. He, Y. You, J. Mo, T. Chen, Controlled synthesis and size effects of multifunctional mesoporous silica nanosystem for precise cancer therapy, Drug Deliv. 25 (1) (2018) 293–306.

[21] K.B. Seljak, P. Kocbek, M. Gašperlin, Mesoporous silica nanoparticles as delivery carriers: an overview of drug loading techniques, J. Drug Delivery Sci. Technol. 59 (2020).

[22] S. Nagappan, A. Mohan, A.M. Thomas, J.M. Yoo, N. Eid, I. Chung, B. Ameduri, C. S. Ha, Synthesis of size-controlled and highly monodispersed silica nanoparticles using a short alkyl-chain fluorinated surfactant, RSC Adv. 11 (4) (2021) 2194–2201.

[23] S.H. Wu, C.Y. Mou, H.P. Lin, Synthesis of mesoporous silica nanoparticles, Chem. Soc. Rev. 42 (9) (2013) 3862–3875.

[24] R.A. Perez, R.K. Singh, T.-H. Kim, H.-W. Kim, Silica-based multifunctional nanodelivery systems toward regenerative medicine, Mater. Horiz. 4 (5) (2017) 772–799.

[25] F. Tang, L. Li, D. Chen, Mesoporous silica nanoparticles: synthesis, biocompatibility and drug delivery, Adv. Mater. 24 (12) (2012) 1504–1534.

[26] V. González-Ruiz, A.I. Olives, M.A. Martín, Core-shell particles lead the way to renewing high-performance liquid chromatography, TrAC Trends Anal. Chem. 64 (2015) 17–28.

[27] R. Hayes, A. Ahmed, T. Edge, H. Zhang, Core-shell particles: preparation, fundamentals and applications in high performance liquid chromatography, J. Chromatogr. A 1357 (2014) 36–52.

[28] R.S. Dubey, Y.B.R.D. Rajesh, M.A. More, Synthesis and characterization of SiO2 nanoparticles via sol-gel method for industrial applications, Mater. Today Proc. 2 (4–5) (2015) 3575–3579.

[29] K. Fuchigami, Y. Taguchi, M. Tanaka, Synthesis of spherical silica particles by sol-gel method and application, Polym. Adv. Technol. 19 (8) (2008) 977–983.

[30] Q. Guo, D. Huang, X. Kou, W. Cao, L. Li, L. Ge, J. Li, Synthesis of disperse amorphous SiO2 nanoparticles via sol–gel process, Ceram. Int. 43 (1) (2017) 192–196.

[31] S.M. Chang, M. Lee, W.S. Kim, Preparation of large monodispersed spherical silica particles using seed particle growth, J. Colloid Interf. Sci. 286 (2) (2005) 536–542.

[32] H. Giesche, Synthesis of monodispersed silica powders II. Controlled growth reaction and continuous production process, J. Eur. Ceram. Soc. 14 (3) (1994) 205–214.

[33] S.-L. Chen, P. Dong, G.-H. Yang, J.-J. Yang, Characteristic aspects of formation of new particles during the growth of monosize silica seeds, J. Colloid Interface Sci. 180 (1) (1996) 237–241.

[34] L. Ernawati, R. Balgis, T. Ogi, K. Okuyama, Tunable synthesis of mesoporous silica particles with unique radially oriented pore structures from tetramethyl orthosilicate via oil-water emulsion process, Langmuir 33 (3) (2017) 783–790.

[35] H. Gustafsson, S. Isaksson, A. Altskar, K. Holmberg, Mesoporous silica nanoparticles with controllable morphology prepared from oil-in-water emulsions, J. Colloid Interface Sci. 467 (2016) 253–260.

[36] B. Zhao, Y. Zhang, T. Tang, F. Wang, T. Li, Q. Lu, Preparation of high-purity monodisperse silica microspheres by the sol–gel method coupled with polymerization-induced colloid aggregation, Particuology 22 (2015) 177–184.

[37] L. Zhao, J.G. Yu, R. Guo, B. Cheng, Preparation and formation mechanisms of monodispersed mesoporous SiO_2 microspheres by the PICA method, Key Eng. Mater. 280 (2004) 1153–1156.

[38] L.P. Singh, S.K. Bhattacharyya, R. Kumar, G. Mishra, U. Sharma, G. Singh, S. Ahalawat, Sol-Gel processing of silica nanoparticles and their applications, Adv. Colloid Interf. Sci. 214 (2014) 17–37.

[39] R. Sumathi, R. Thenmozhi, Synthesis and characterization of spherical silica nanoparticles by sol-gel method, Int. Conf. Syst. Sci. Control Commun. Eng. Technol. (2015) 204–208.

[40] W. Stöber, A. Fink, E. Bohn, Controlled growth of monodisperse silica spheres in the micron size range, J. Colloid Interface Sci. 26 (1) (1968) 62–69.

[41] X. Luo, J. Dong, L. Zhang, J. Du, H. Wang, W. Gao, Preparation of silica micro spheres via a semibatch sol–gel method, J. Sol.-Gel. Sci. Technol. 81 (3) (2016) 669–677.

[42] S.-L. Chen, Preparation of monosize silica spheres and their crystalline stack, Colloids Surf. A Physicochem. Eng. Asp 142 (1) (1998) 59–63.

[43] H. Nakabayashi, A. Yamada, M. Noba, Y. Kobayashi, M. Konno, D. Nagao, Electrolyte-added one-pot synthesis for producing monodisperse, micrometer-sized silica particles up to 7 microm, Langmuir 26 (10) (2010) 7512–7515.

[44] H. Gustafsson, K. Holmberg, Emulsion-based synthesis of porous silica, Adv. Colloid Interf. Sci. 247 (2017) 426–434.

[45] Y. Bao, C. Shi, T. Wang, X. Li, J. Ma, Recent progress in hollow silica: template synthesis, morphologies and applications, Micropor. Mesopor. Mater. 227 (2016) 121–136.

[46] T. Koźlecki, I. Polowczyk, A. Bastrzyk, W. Sawiński, Improved synthesis of nanosized silica in water-in-oil microemulsions, J. Nanopart. 2016 (2016) 1–9.

[47] H. Ono, K. Takahashi, Preparation of silica microcapsules by sol-gel method in W/O emulsion, J. Chem. Eng. Jpn. 31 (5) (1998) 808–812.

[48] Q. Chen, J. Larismaa, A. Keski-Honkola, K. Vilonen, O. SÖDerberg, S.-P. Hannula, Effect of synthesis time on morphology of hollow porous silica microspheres, Mater. Sci. 18 (1) (2012), https://doi.org/10.5755/j01.ms.18.1.1344.

[49] D. Trunov, F. Muzika, A. Kříž, J. Štětina, I. Sedlářová, M. Dendisová, F. Hassouna, M. Šoóš, Ambient-temperature porogen-free method for preparation of silica-based macroporous materials, Colloids Surf. A Physicochem. Eng. Asp 634 (2022).

[50] T. Schmidts, D. Dobler, C. Nissing, F. Runkel, Influence of hydrophilic surfactants on the properties of multiple W/O/W emulsions, J. Colloid Interf. Sci. 338 (1) (2009) 184–192.

[51] W.-X. SiTu, H.-M. Lu, C.-Y. Ruan, L. Zhang, Y. Zhu, L. Zhang, Effect of polymer on dynamic interfacial tensions of sulfobetaine solutions, Colloids Surf. A Physicochem. Eng. Asp 533 (2017) 231–240.

[52] Y. Lu, W. Kang, J. Jiang, J. Chen, D. Xu, P. Zhang, L. Zhang, H. Feng, H. Wu, Study on the stabilization mechanism of crude oil emulsion with an amphiphilic polymer using the β-cyclodextrin inclusion method, RSC Adv. 7 (14) (2017) 8156–8166.

[53] K.M. Koczkur, S. Mourdikoudis, L. Polavarapu, S.E. Skrabalak, Polyvinylpyrrolidone (PVP) in nanoparticle synthesis, Dalton Trans. 44 (41) (2015) 17883–17905.

[54] K. Wanli, L. Yi, Q. Baoyan, L. Guangzhi, Y. Zhenyu, H. Jichun, Interactions between alkali/surfactant/polymer and their effects on emulsion stability, Colloids Surf. A Physicochem. Eng. Asp 175 (1–2) (2000) 243–247.

[55] W. Kang, B. Xu, Y. Wang, Y. Li, X. Shan, F. An, J. Liu, Stability mechanism of W/O crude oil emulsion stabilized by polymer and surfactant, Colloids Surf. A Physicochem. Eng. Asp 384 (1–3) (2011) 555–560.

[56] T. Dreher, J. Glass, A. O'Connor, G. Stevens, Effect of rheology on coalescence rates and emulsion stability, AIChE J. 45 (6) (1999) 1182–1190.

[57] J. Reimers, F. Schork, Predominant droplet nucleation in emulsion polymerization, J. Appl. Polym. Sci. 60 (2) (1996) 251–262.

[58] I. Rahman, P. Vejayakumaran, C. Sipaut, J. Ismail, M.A. Bakar, R. Adnan, C. Chee, An optimized sol–gel synthesis of stable primary equivalent silica particles, Colloids Surf. A Physicochem. Eng. Asp 294 (1–3) (2007) 102–110.

[59] W. Wan, Y. Feng, J. Yang, S. Xu, T. Qiu, Preparation of mesoporous silica ceramics with relatively high strength from industrial wastes by low-toxic aqueous gel-casting, J. Eur. Ceram. Soc. 35 (7) (2015) 2163–2170.